Supporting Information for Publication

Regulating the Heteroatom Doping in Metallogel-derived Co@Dual Self-doped Carbon Onions to Maximize Electrocatalytic Water Splitting

Ekata Saha,[a,b] Kannimuthu Karthick,[b,c] Subrata Kundu,[b,c,*] Joyee Mitra[a,b,*]

[a] Ms. Ekata Saha, Dr. Joyee Mitra

Inorganic Materials & Catalysis (IMC) Division, CSIR-Central Salt & Marine Chemicals Research Institute, Gijubhai Badheka Marg, Bhavnagar-364002, Gujarat, India.

E-mail: joyeemitra@csmcri.res.in, joyeemitra@gmail.com

[b]Academy of Scientific and Innovative Research (AcSIR), AcSIR Headquarters, CSIR-HRDC Campus, Sector-19, Kamla Nehru Nagar, Ghaziabad-201002, U.P., India.

[c] Mr. Kannimuthu Karthick, Dr. Subrata Kundu
Electrochemical Process Engineering (EPE) Division, CSIR-CECRI, Karaikudi, Tamil Nadu-630003.

E-mail: skundu@cecri.res.in, kundu.subrata@gmail.com

Tables: 2 (S1-S2)

Figures: 17 (S1-S17)

Total pages: 24 (S1- S25)

Index:

EXPERIMENTAL SECTION

Instrumentation and Chemicals.

All reagents and solvents were commercially available and used as received without further purification. N,N-Dimethylformamide (DMF), Cobalt(II) acetate tetrahydrate [$Co(OAc)_2.4H_2O$] and 3,5-diamino-1,2,4-traizole were procured from Finar Chemicals, Fisher Scientific and Sigma Aldrich respectively and used as received. The synthesized metallo-organogel and corresponding xerogel derived materials were characterized using several techniques such as PXRD, FT-IR, FT-Raman, TEM, SEM, BET-Surface area and XPS analyses. The powder X-ray diffraction (PXRD) analysis was done using Philips X'pert MPD system (PANalytical diffractometer) with Cu $K_{\alpha 1}$ radiation (λ = 0.154 nm). The diffraction pattern was measured in the 2θ range from 5-80° at an operating voltage of 40 kV, 30 mA current, with a scan speed of 3º min^{-1} and a step size of 0.013º in 2θ at RT with a scan step time 58.395 sec. Anode material was Cu and the value of $K_{\alpha 1}$, $K_{\alpha 2}$ and K_{β} were 1.54060 [Å], 1.54443 [Å] and 1.39225 [Å] respectively. Fourier transform Infrared Spectra analysis (FT-IR) was recorded on Perkin Elmer-Spectrum G-FTIR spectrometer (Germany) from 400-4000 cm^{-1} with a resolution of 4 cm^{-1} using KBr pellets. The FT-Raman spectra were collected on a LabRAM HR Evolution Raman Spectrometer with a 532 nm laser source. The surface morphology of prepared gel material was analyzed by Field Emission- Scanning Electron Microscope (FE-SEM) (JEOL JSM 7100F) with an accelerating voltage of 5–15 kV with 10 μA of emission current. The transition electron microscope (TEM) analysis was done with JEOL, JEM 2100 TEM instrument. XPS analysis was recorded with Omicron ESCA (Oxford Instruments, Germany) instruments. N_2 adsorption isotherms of the materials were recorded using a Micromeritics ASAP 2020 analyzer. The surface area of the samples was obtained from the Brunauer-Emmett-Teller (BET) surface area analysis using N_2 adsorption/ desorption isotherm data. The samples were pretreated by degassing at 180 °C for 6 hours before the measurements. The pore volume data was calculated by using the BJH method for calculating the pore size distribution using the Kelvin equation and DH methods.

Post OER structural characterizations are carried out using the following instruments. The X-ray diffraction (XRD) analysis was carried out by a PAN analytical Advanced Bragg-Brentano X-ray powder diffractometer (XRD) with Cu K_{α} radiation (λ = 0.154178 nm) with a scanning rate of 5° min^{-1} in the 2θ range 10-80°. The microstructural studies and HAADF color mapping were carried out in HR-TEM, (Tecnai TM G2TF20) working at an accelerating voltage of 200 kV. The Energy Dispersive X-ray Spectroscopy (EDS) analysis was done with

the HR-TEM with a separate EDS detector (INCA) connected to that instrument. The Scanning Electron Microscope (SEM) analysis as done with Tescan VEGA 3 SBH instrument with Bruker Easy EDS attached setup. The X-ray photoelectron spectroscopic (XPS) analysis was analyzed by using Theta Probe AR-XPS System, Thermo Fisher Scientific (U.K). The X-ray fluorescence (XRF) analysis was carried out using XGT-5200 X-ray analytical microscope with X-ray tube 50 kV max, 1 mA, with Rh target (0-40 keV).

Materials Synthesis.

CoGel. A hot DMF solution (2 mL) of DAT (0.25 mmol, 0.025 g) was prepared in a 5 mL capped glass vial. Then $Co(OAc)_2.4H_2O$ (0.25 mmol, 0.06 g) was added to that DAT solution. Then the reaction mixture was stirred at RT for 20 minutes. After this time, a violet-colored gel (**CoGel**) was obtained. The gelation state of the material was primarily observed by "stable-to-inversion" test of the glass vial.

N-doped Carbon@CoNPs. The as synthesized CoGel was dried in hot air oven at 70°C for 4 days to obtain a violet-colored powder material called Co-xerogel. Then the violet-colored powder material was calcined at 500 and 800°C for 6 hours under N_2 atmosphere to obtain the sample "**EK-a**" and "**EK-b**" respectively. Similarly, the violet colored xerogel was again calcined at 800°C for 6 hours under mixed gas (95% Ar + 5% H_2) atmosphere to obtain the sample "**EK-c**".

Co@CoO@Co_3O_4-decorated N-doped Carbon. The as synthesized sample **EK-c** was calcined at 250°C for 0.5 hour in a muffle furnace (in air) to obtain the sample "**EK-d**".

Preparation of samples (catalysts) for Electrocatalytic OER

The electrocatalytic OER study was carried out with the as synthesized materials **EK-a**, **EK-b**, **EK-c** and **EK-d**. The catalytic ink was prepared by taking 3 mg of each catalyst dispersed in 1 mL of solution that contains 750 μL H_2O, 250 μL ethanol and 50 μL of nafion. After this, the solution was sonicated for 15 minutes for the complete dispersion of the catalyst. Then, 34.5 μL of solution was drop-casted to the carbon cloth (CC) substrate corresponding to the area of 1×0.5 cm^2 and the studies were normalized to 1×0.5 cm^2. Hence, the normalized loading of a catalyst becomes ~0.205 mg cm^{-2}. After having drop-casted into the conducting substrate (CC), it was allowed to dry at room temperature. The prepared electrodes were next subjected to electrocatalytic OER study in 1 M KOH. The polarization studies are carried out at 5 mV S^{-1} and 50 % *iR* compensated. EIS studies are carried out at an overpotential of 444

mV in the frequency region of 100 kHz to 0.1 Hz with an amplitude potential of 0.05 V. The robustness of the catalysts was analysed at high scan rate of 200 mV s^{-1} for 500 cycles and potentiostatic (PSTAT) analysis was carried out for 12 h at an overpotential of 474 mV without any iR compensation. All the electrochemical data acquired using Hg/HgO reference electrode is converted into RHE scale.

The efficiency of our catalysts is comparable with the previously reported Co containing carbon materials. Here we are providing a list of overpotential observed of different Co based carbon systems at 10 mA cm^{-2} for OER (**Table S1**).

Table-S1: Comparison between literature reported overpotential with the data reported in this paper

Sl. No.	Catalytic System Used	Overpotential / mV	Reference
1.	N/O-dual doped carbon coated CoNPs (EK-a)	413	*This work*
2.	N/O-dual doped carbon coated CoNPs (EK-b)	378	*This work*
3.	N/O-dual doped carbon coated CoNPs (EK-c)	384	*This work*
4.	Co@CoO@Co_3O_4-decorated N/O-dual doped carbon (EK-d)	397	*This work*
5.	Co@mesostructured N-doped Carbon	373	1
6.	Co_3O_4/N-rmGO	310	2
7.	Co-NDC	388	3
8.	NC@Co-NGC DSNCs	410	4
9.	N-CG–CoO	340	5
10.	Co-N_x/C NRA	300	6
11.	Co_xO_y/NC	430	7
12.	Co_3O_4/carbon porous	290	8
13.	Co-CoO/N-rGO	390	9
14.	ECPT-Co@C	450	10
15.	Co_3O_4/CNT	511	11
16.	Co-CN SS	340	12
17.	Co@NC	390	13
18.	Co@N – C	400	14

FTIR spectra of the synthesized cobalt materials under varying pyrolysis conditions

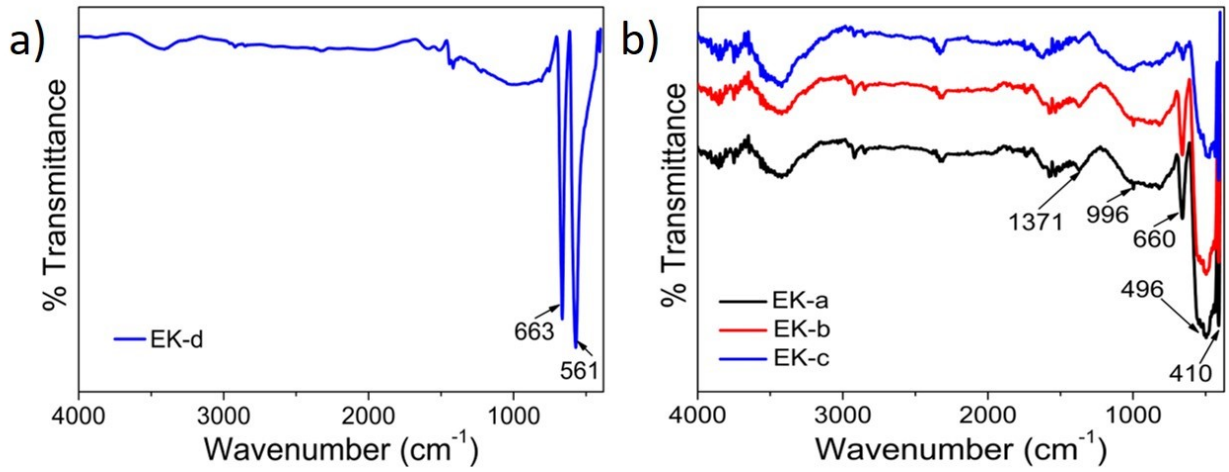

Figure S1. FT-IR spectra of the catalysts a) EK-d and b) EK-a, EK-b and EK-c respectively.

BET Surface area: Nitrogen adsorption desorption isotherms of the synthesized cobalt materials under varying pyrolysis conditions

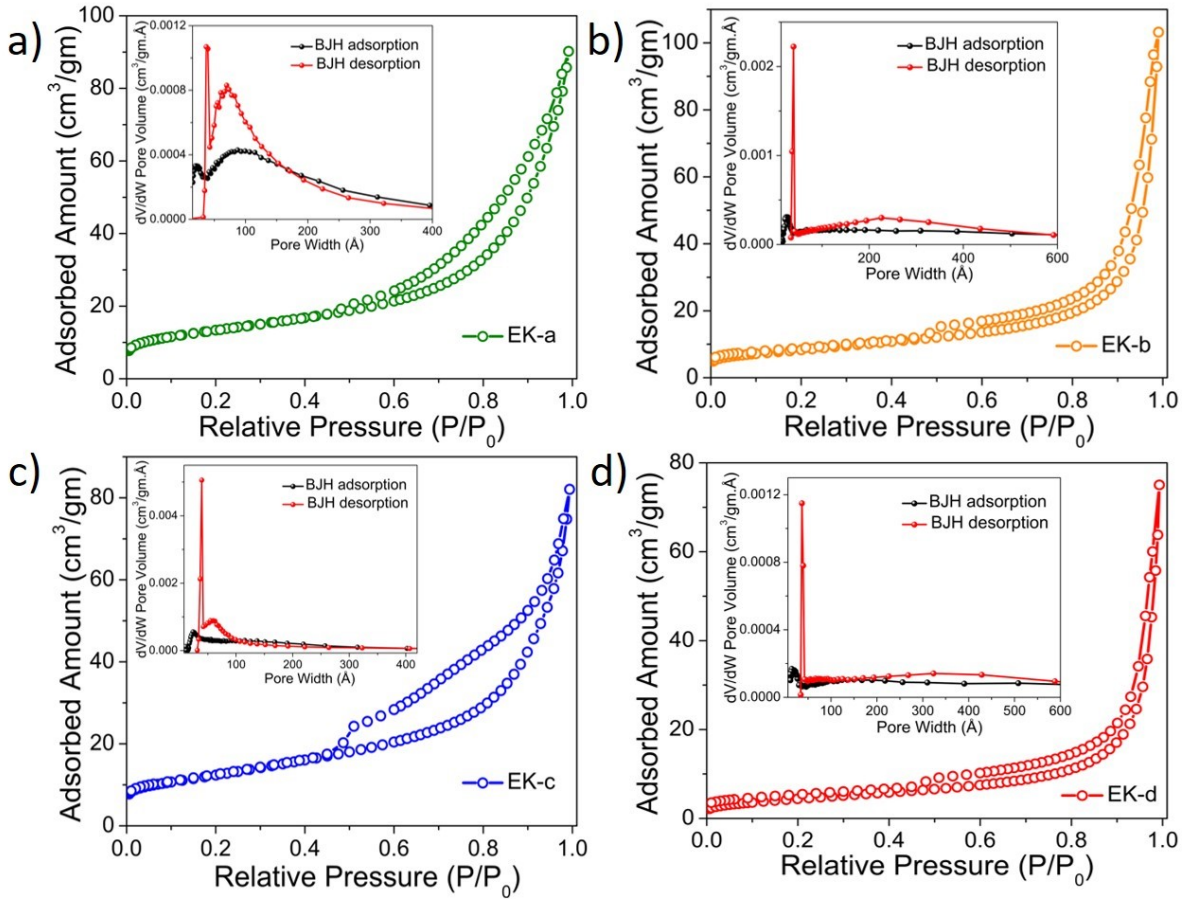

Figure S2. Nitrogen adsorption and desorption isotherms of a) EK-a, b) EK-b, c) EK-c and d) EK-d respectively; the insets show the corresponding BJH pore size distributions.

XPS Results

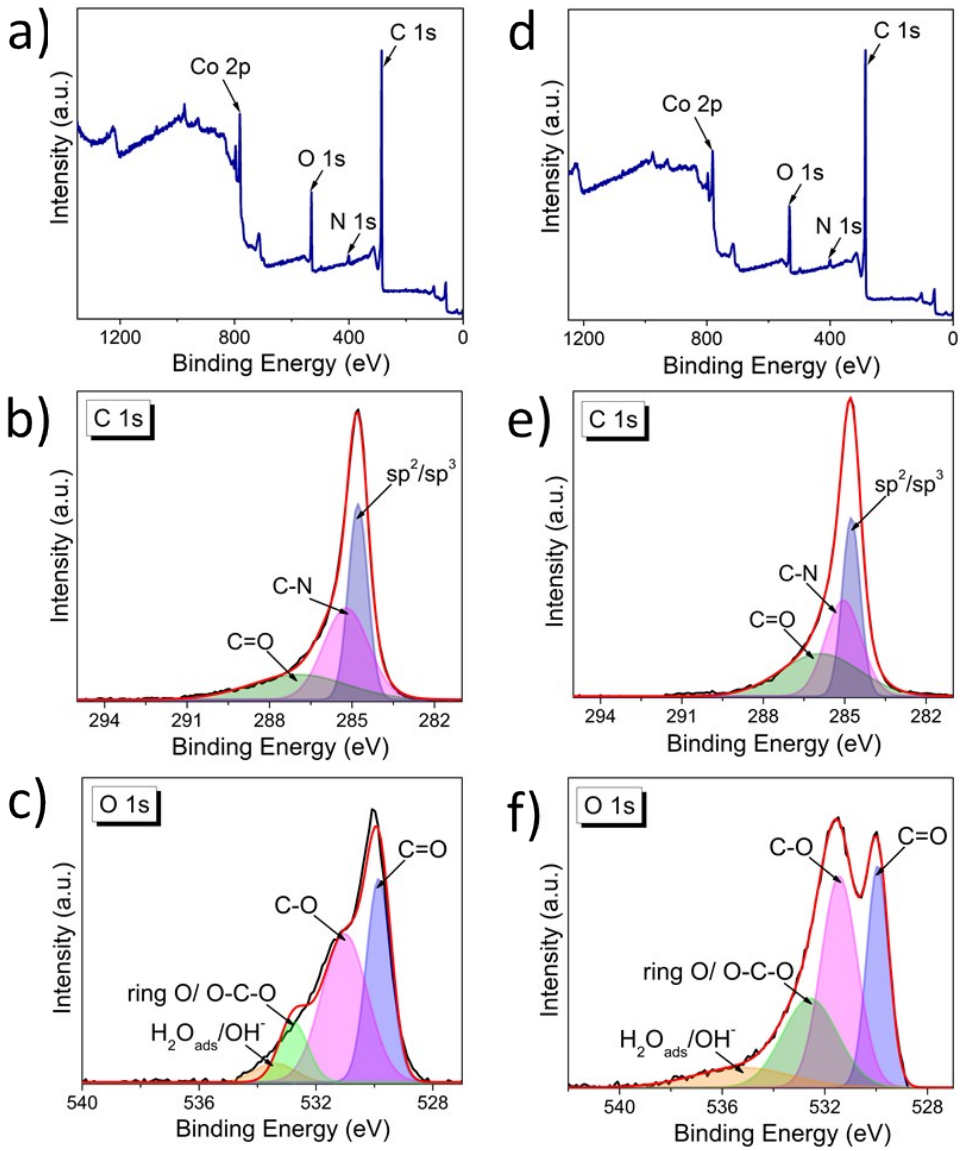

Figure S3. a) and d) depicts the XPS survey spectra, b) and e) shows the high resolution C 1s spectra and c) , f) shows the high resolution O 1s spectra of EK-b and EK-c respectively.

Table-S2: Atomic % of elements in EK-b and EK-c from XPS

Name of the Samples	Atomic%			
	C 1s	Co 2p	O 1s	N 1s
EK-b	81.45	3.79	10.98	3.77
EK-c	81.74	3.78	10.96	2.98

SEM analysis of the cobalt nanomaterials encapsulated within N, O-dual doped carbon onions

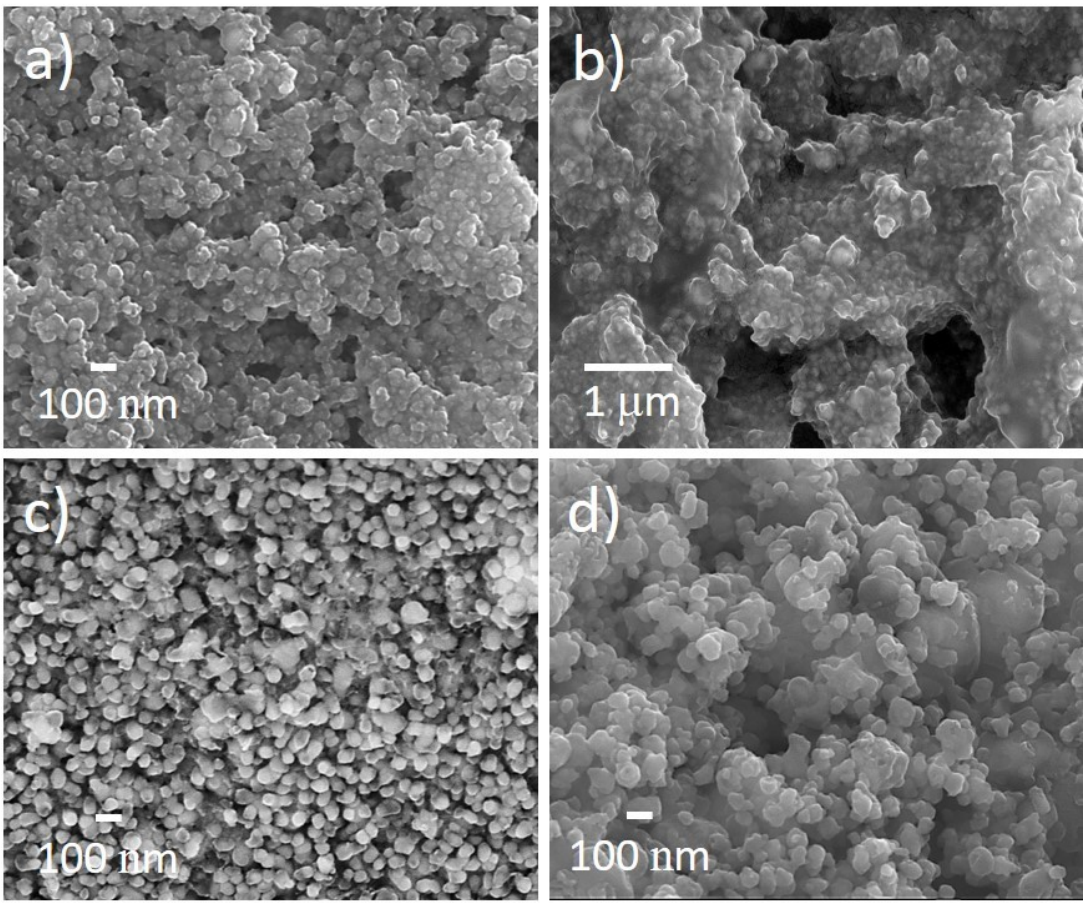

Figure S4. SEM images of the as-synthesized cobalt nanoparticles in a) **EK-a**, b) **EK-b**, c) **EK-c** and interlinked cobalt and cobalt oxide species in d) **EK-d**.

Particle size distribution of the as-synthesized samples from TEM

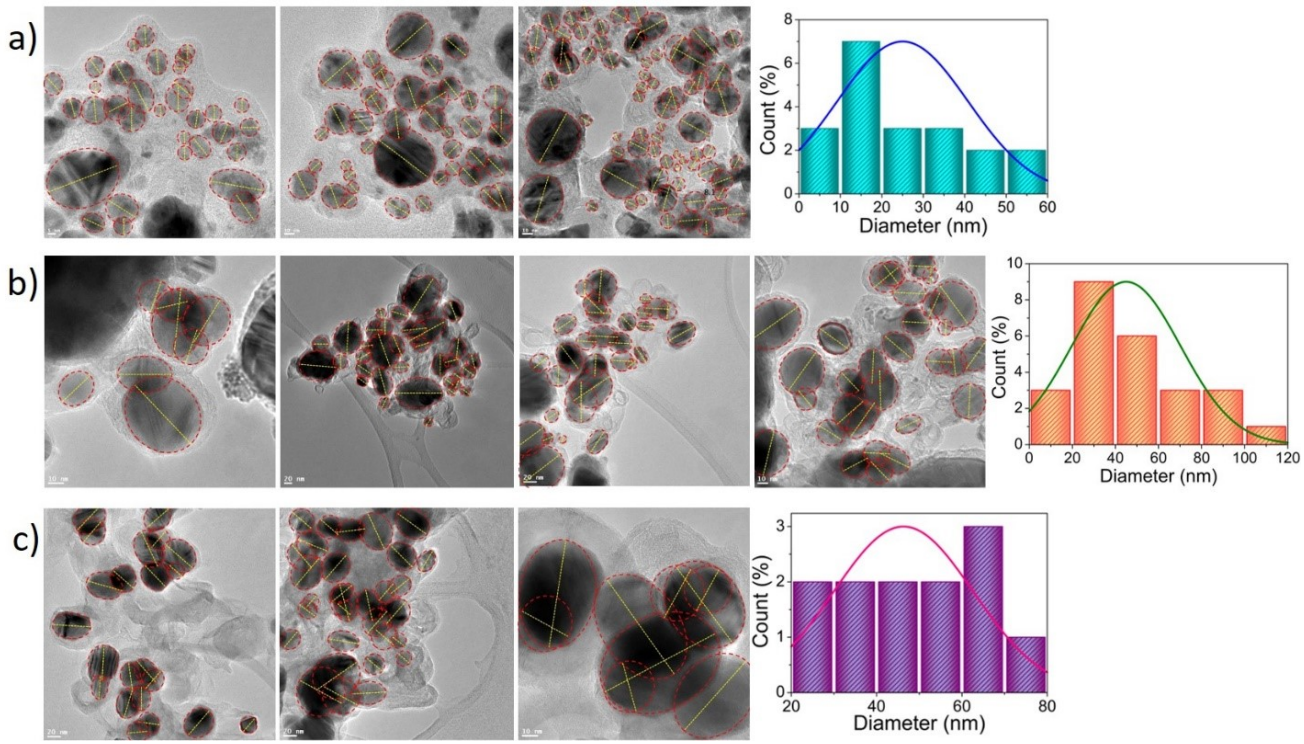

Figure S5. Particle size distribution of the cobalt nanoparticles a) **EK-a**, b) **EK-b** and c) **EK-c** encapsulated in N, O-dual doped carbon onions.

HRTEM analysis of the cobalt nanomaterials encapsulated within N, O-dual doped carbon onions

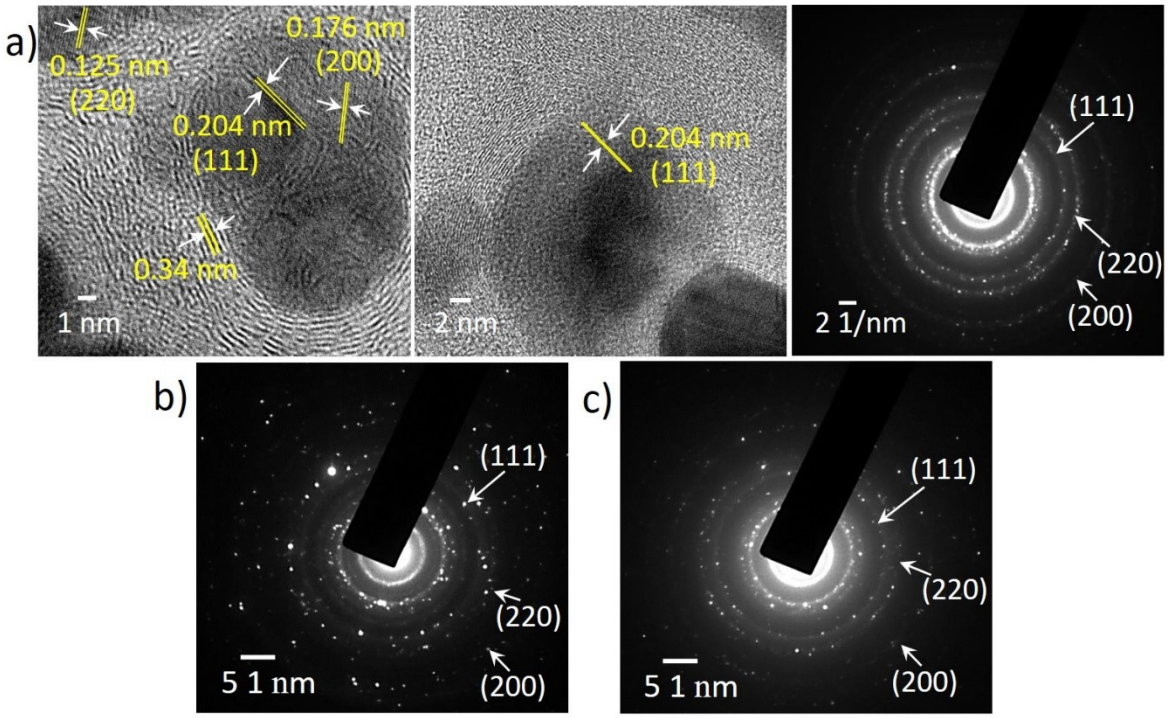

Figure S6. HRTEM images and the corresponding SAED patterns showing carbon onion encapsulated cobalt nanoparticles and the typical lattice planes of metallic cobalt in a) **EK-a**. b) and c) shows the SAED patterns and lattice planes of metallic cobalt in **EK-b** and **EK-c** respectively.

HRTEM analysis of the interlinked sheets of the coexisting cobalt and cobalt oxide phases on doped carbon

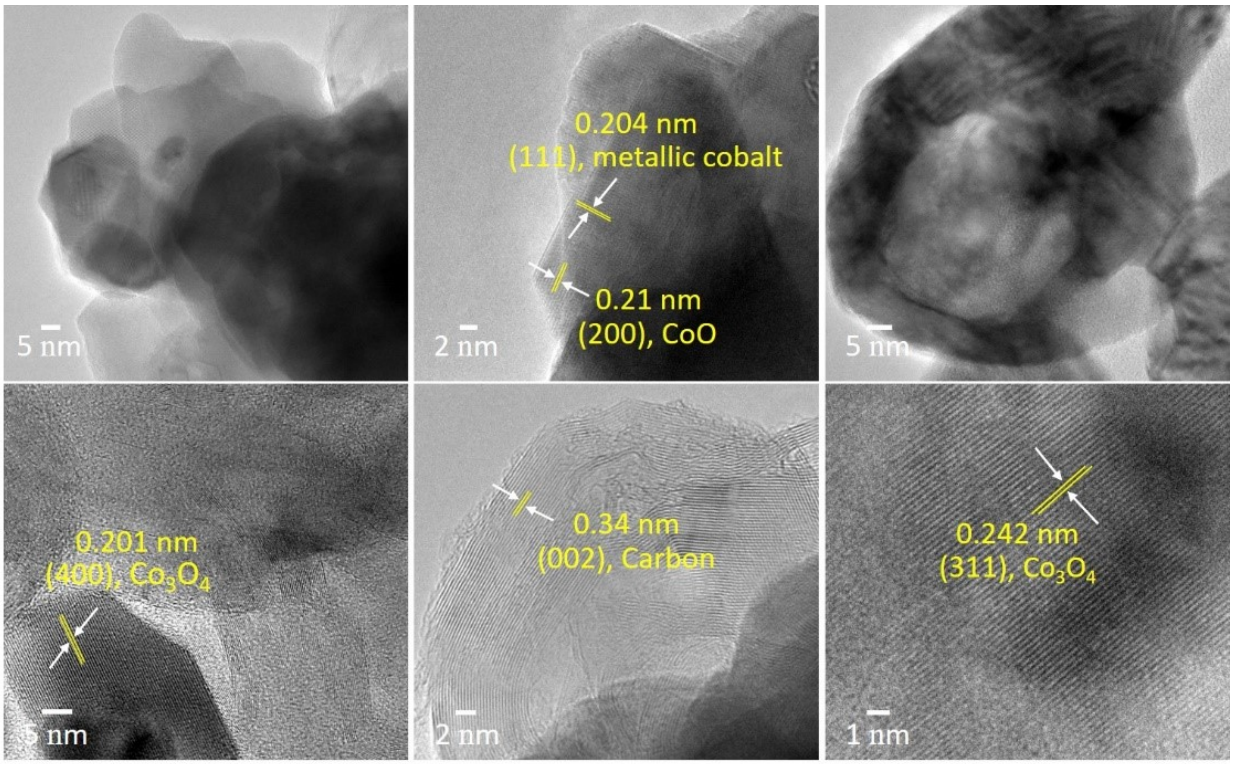

Figure S7. HRTEM images showing nanoparticles decorated interlinked sheet-like morphology and the typical lattice planes of Co@CoO@Co_3O_4-decorated carbon material in the sample **EK-d**.

C_{dl} plots of the cobalt-based electrocatalysts before and after cycling studies

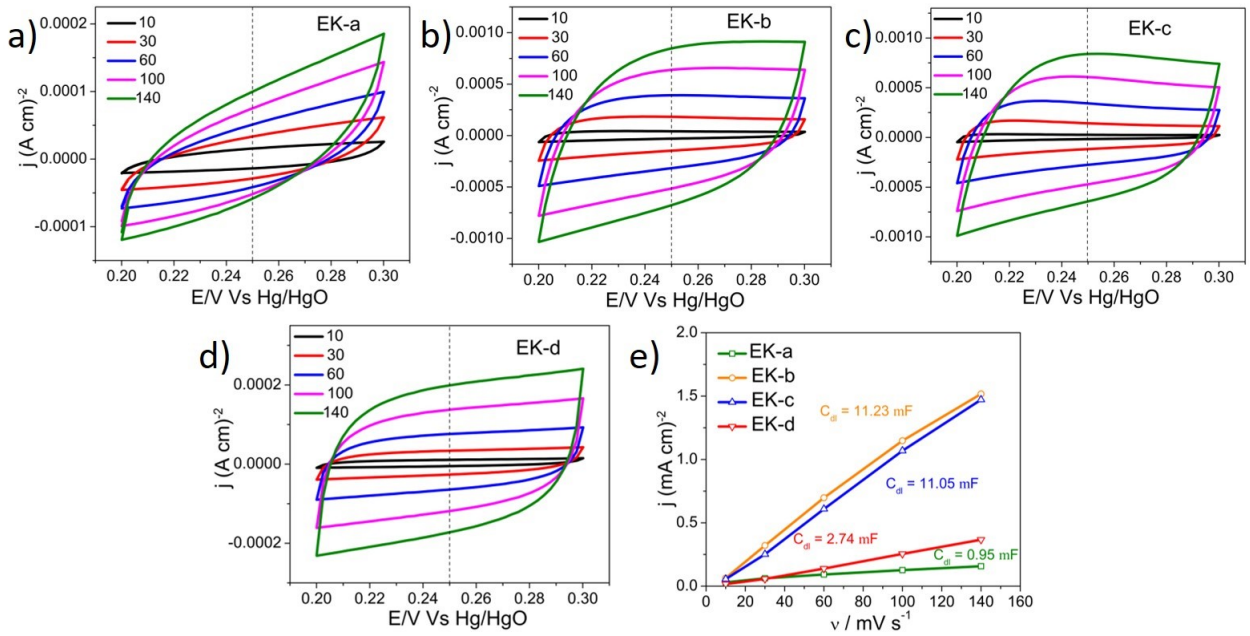

Figure S8. a-d) are the C_{dl} plots of **EK-a**, **EK-b**, **EK-c** and **EK-d** at C_{dl} regions. e) Corresponding C_{dl} values of each catalysts at different scan rates.

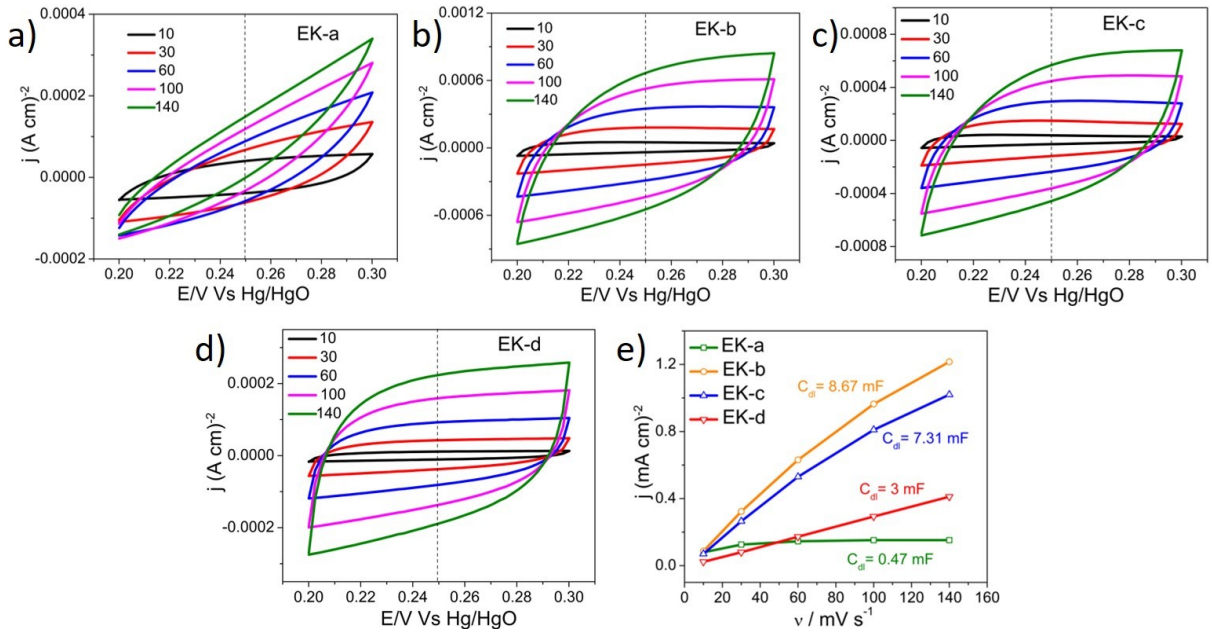

Figure S9. a-d) are the C_{dl} plots of **EK-a**, **EK-b**, **EK-c** and **EK-d** at C_{dl} regions after cycling study. e) Corresponding C_{dl} values of each catalysts at different scan rates.

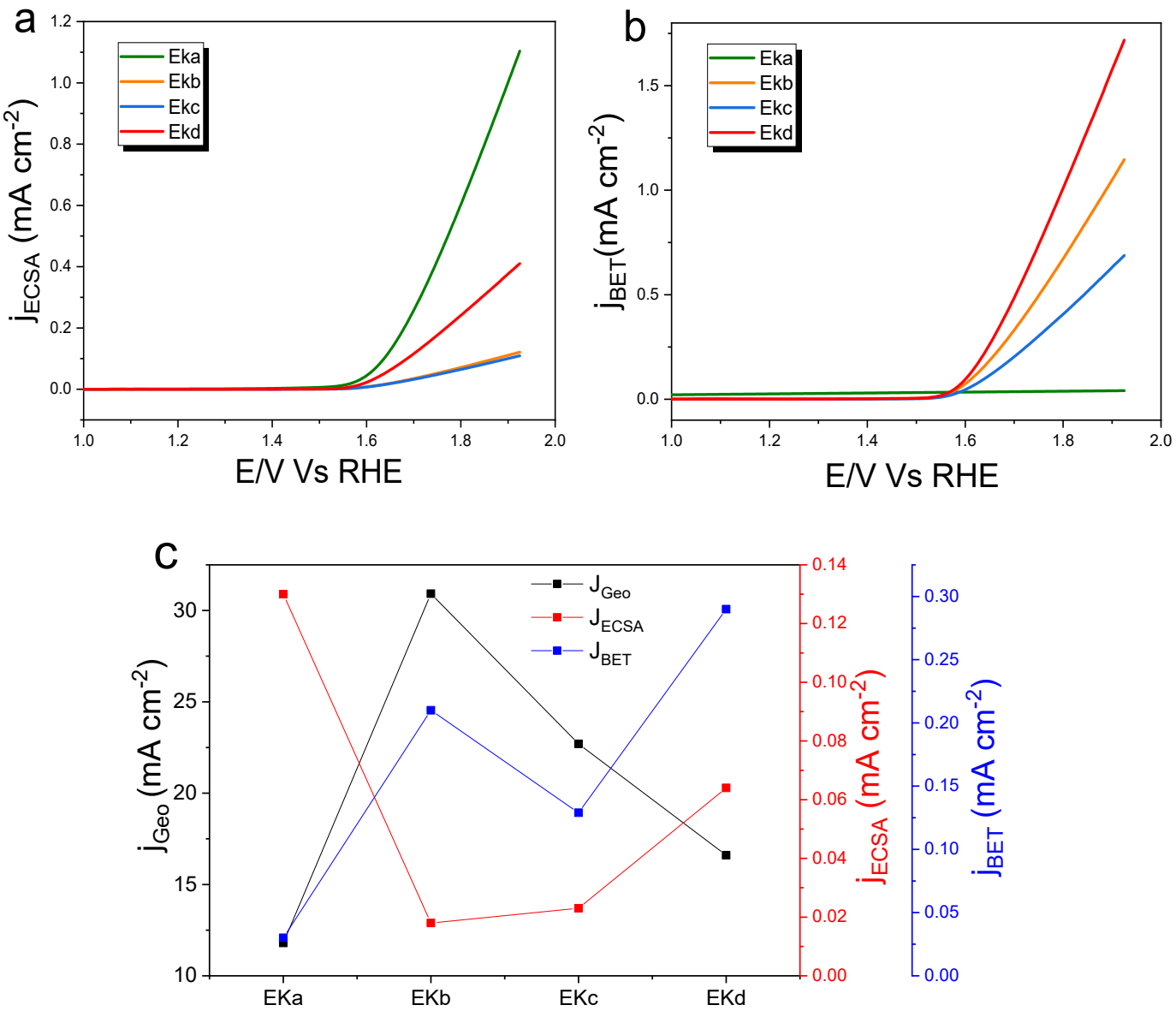

Figure S10. a and b) are the ECSA and BET normalized currents of EK-a, EK-b, EK-c and EK-d and c) is the comparison of j_{geo}, j_{ECSA} and j_{BET} normalized currents of all the catalysts at 1.65 V respectively.

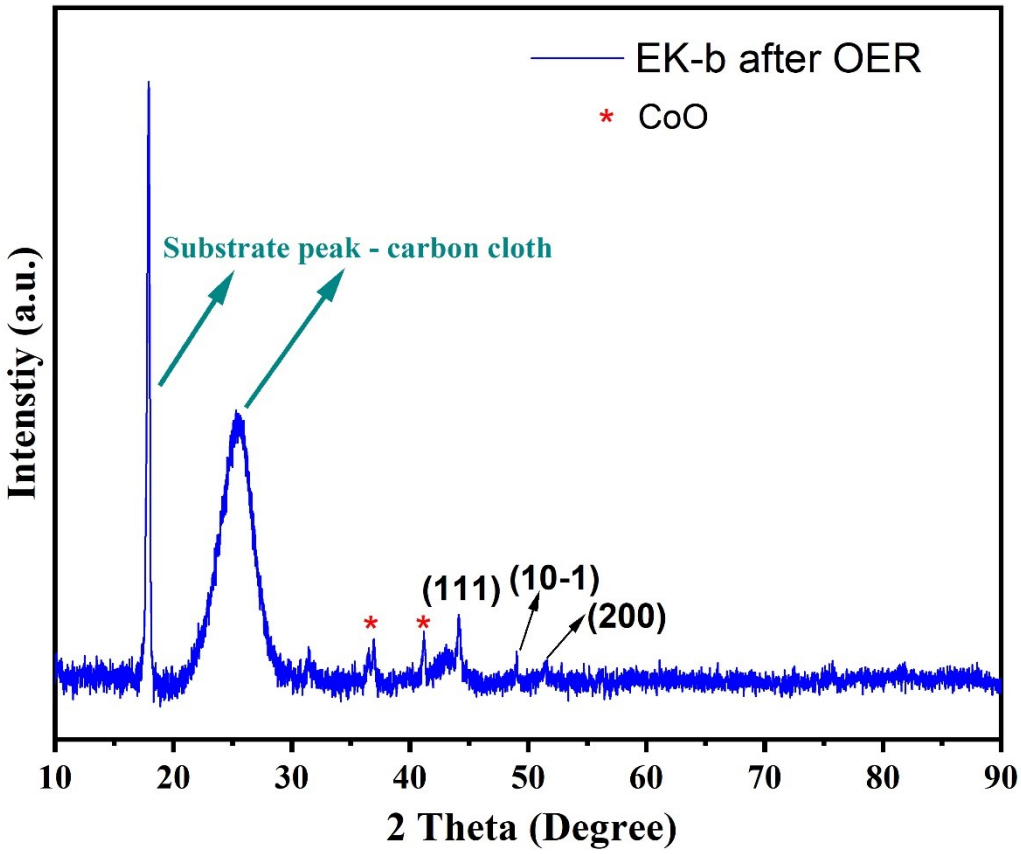

Figure S11. Post OER XRD results of **EK-b** showing the presence of Co and CoO after the OER study.

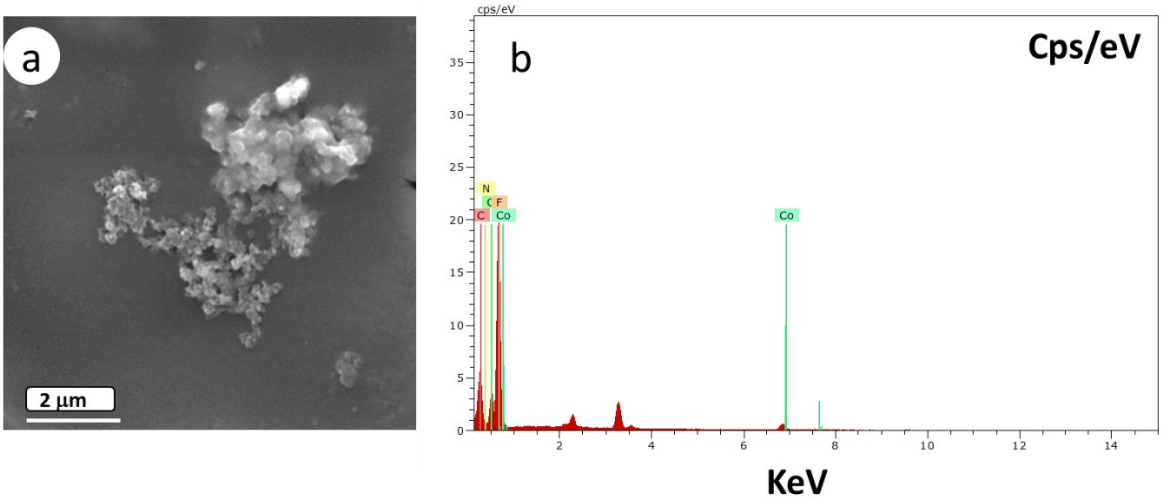

Figure S12. a) Post OER SEM image of **EK-b**, and b) corresponding EDS pattern showing the presence of Co, N, C and O.

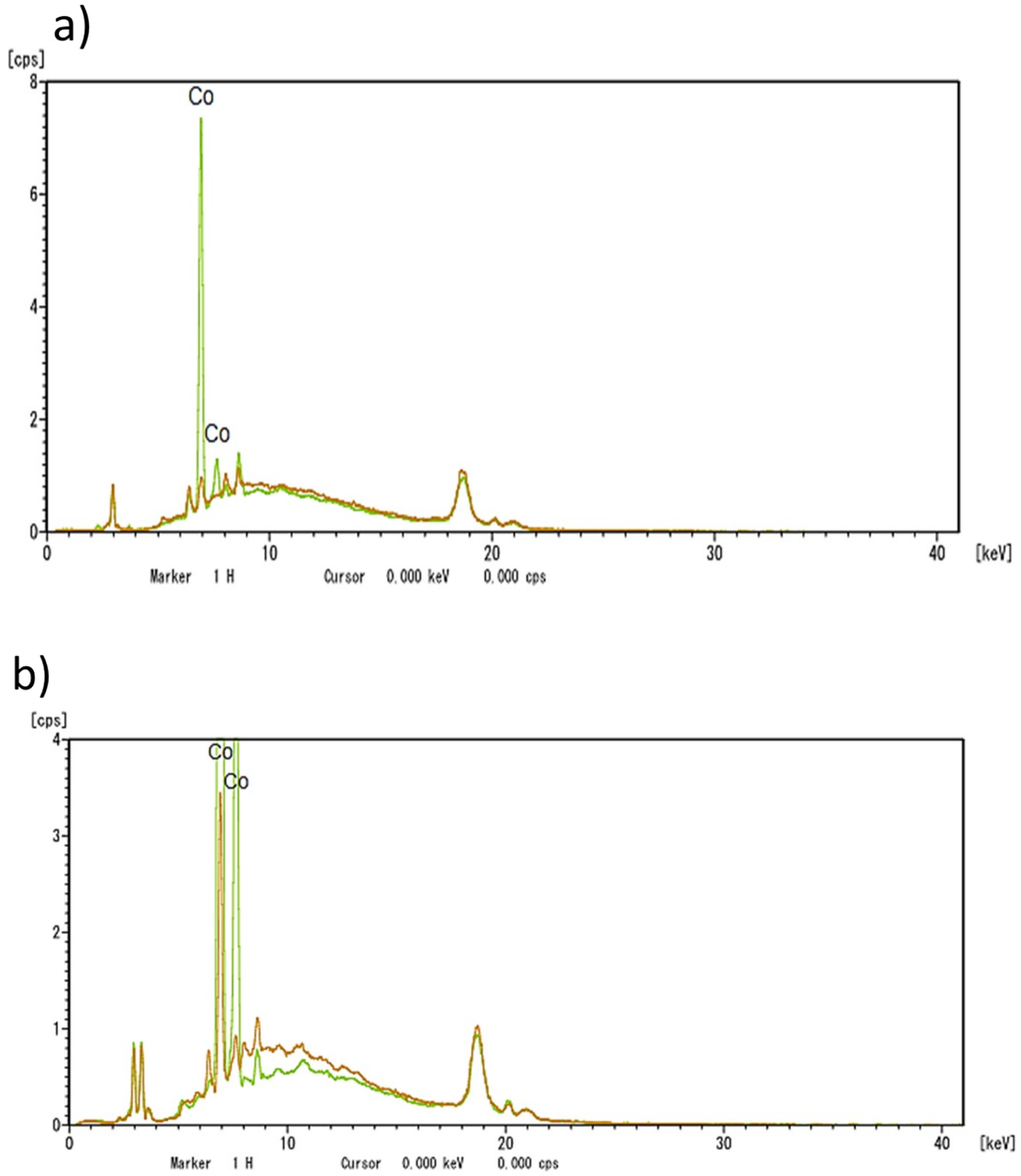

Figure S13. (a) and (b) are the Pre and post OER XRF analysis of **EK-b** showing the presence of Co and inferring the stability of the electrodes.

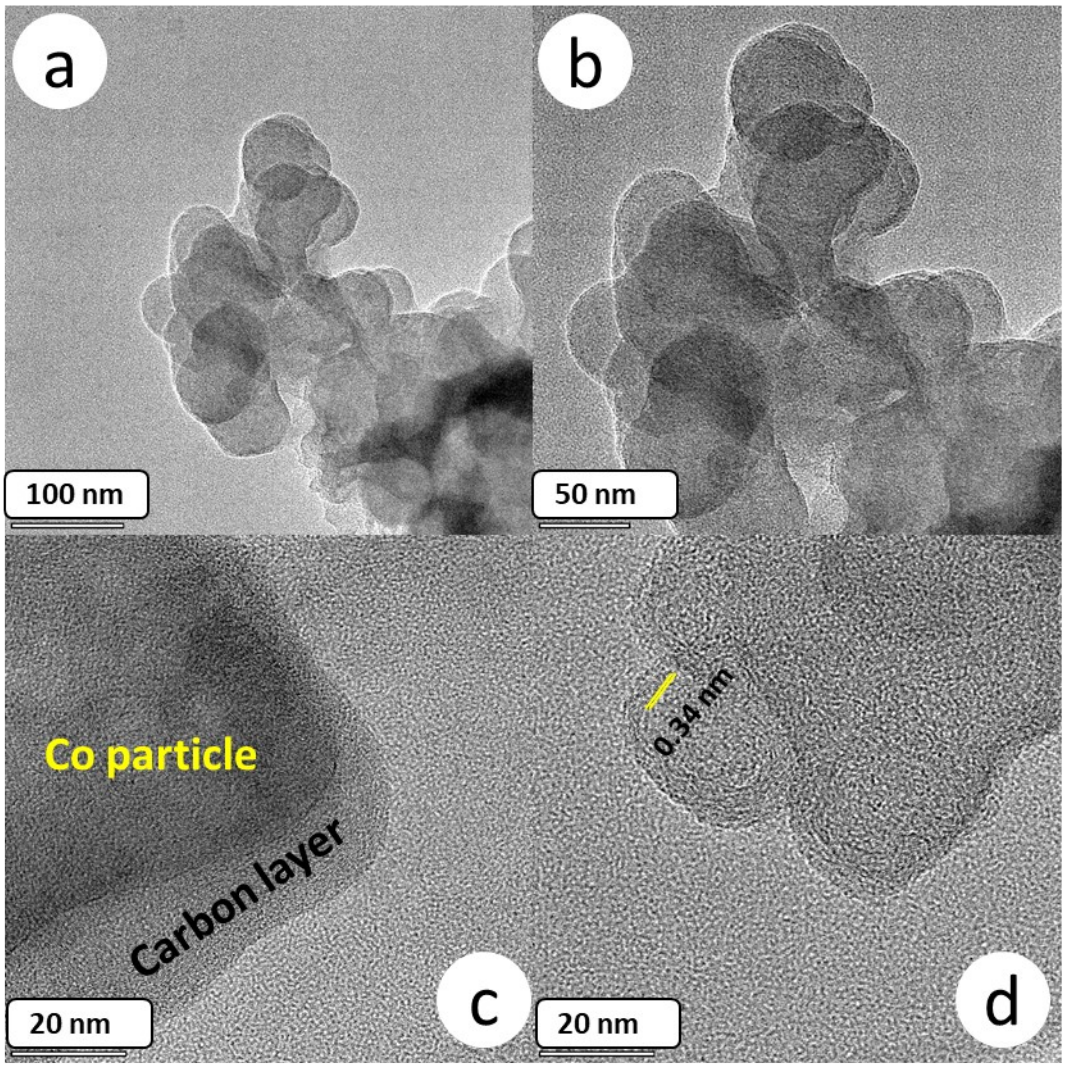

Figure S14. (a-d) Post OER HR-TEM images of **EK-b** from low to high-magnification with the presence of stable carbon onion layers.

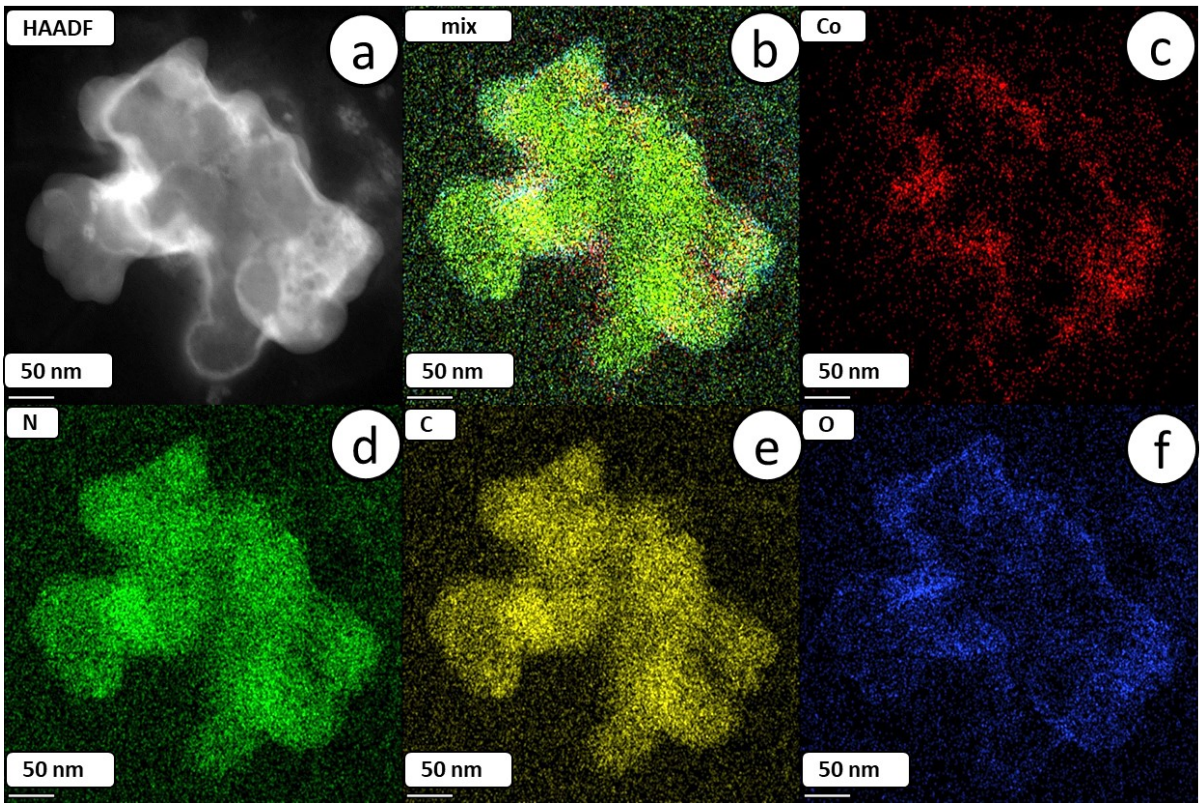

Figure S15. (a-f) Post OER HR-TEM HAADF color mapping images of **EK-b** for area chosen, mix, Co, N, C and O respectively.

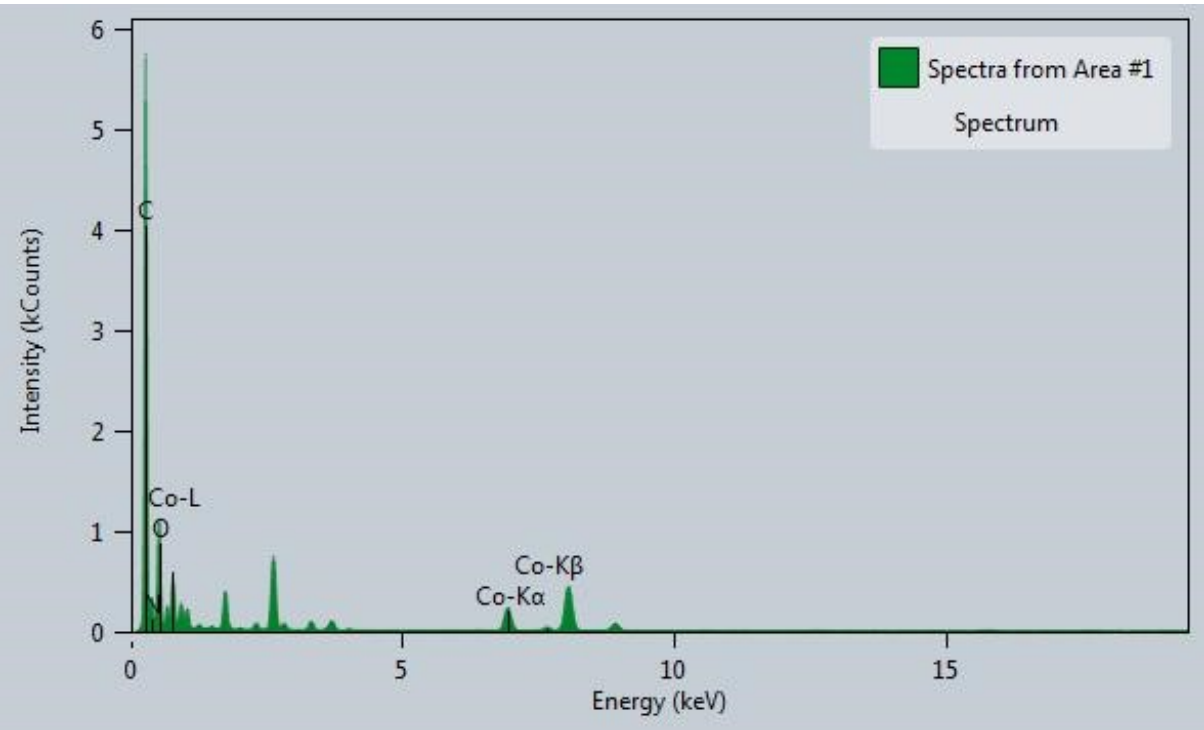

Figure S16. Post OER HR-TEM EDS images of **EK-b** showing the presence of Co, N, C and O respectively.

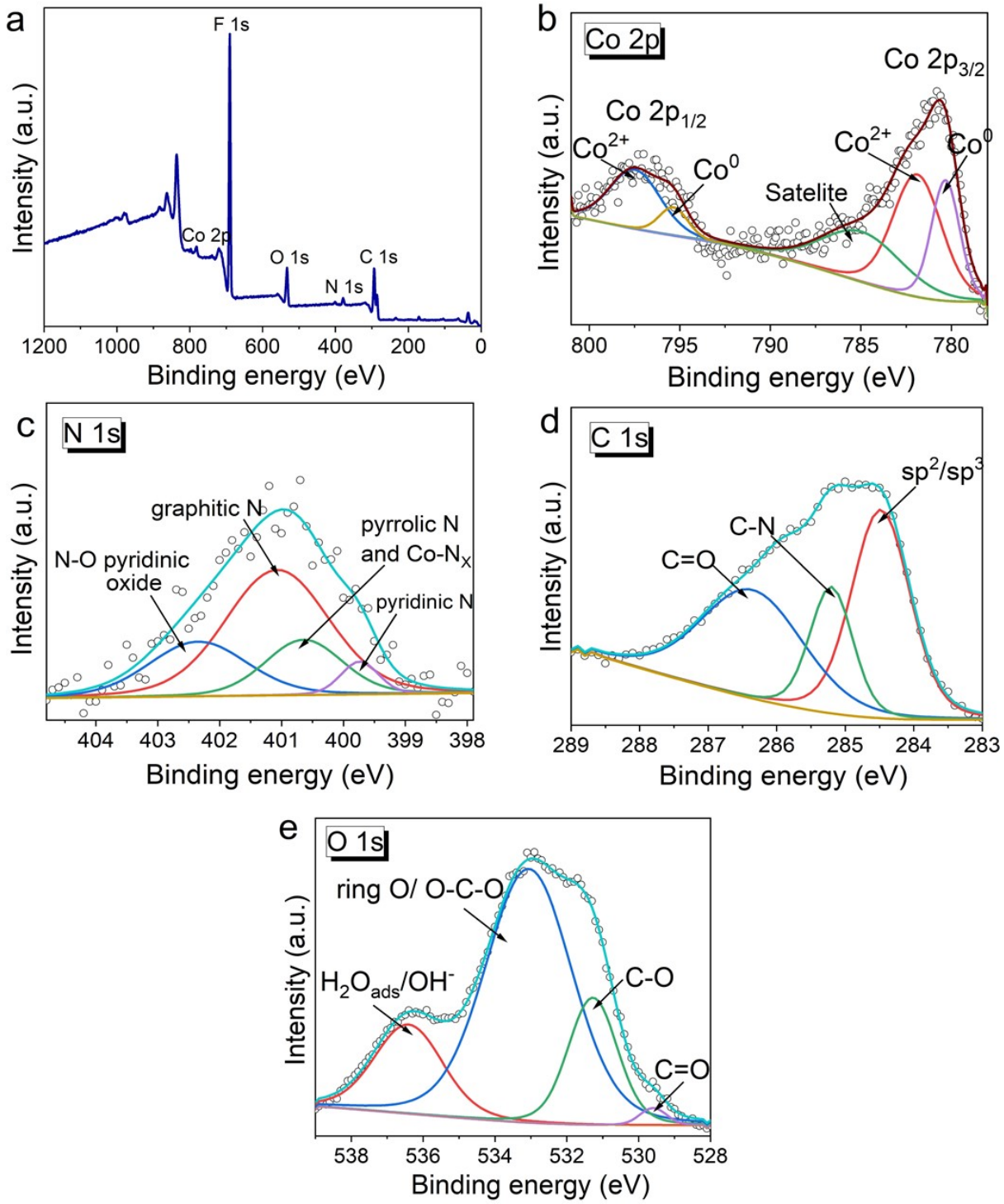

Figure S17. (a-e) Post OER XPS results of **EK-b** for survey spectrum, Co 2p, N 1s, C 1s and O 1s respectively.

ECSA calculation

$$ECSA = C_{dl}/C_s$$

Here, C_s is the specific capacitance of a flat surface and from the references of the previous reports, we have used the value of 0.040 mF cm^{-2} ***(J. Am. Chem. Soc. 2015, 137, 4347−4357)***.

For, **EK-a**, ECSA = 0.95/0.040 = 23.75 cm^2

For, **EK-b**, ECSA = 11.23/0.040 = 280.75 cm^2

For, **EK-c**, ECSA = 0.95/0.040 = 276.25 cm^2

For, **EK-d**, ECSA = 0.95/0.040 = 68.5 cm^2

For roughness factor

R_f = ECSA/geometrical area of the working electrode

For, **EK-a**, R_f = 23.75 /0.5 = 47.5 cm^2

For, **EK-b**, R_f = 280.75 /0.5= 561.5 cm^2

For, **EK-c**, R_f = 276.25 /0.5 = 553 cm^2

For, **EK-d**, R_f = 68.5/0.5= 137 cm^2

For TOF calculation

TOF = jM/4mF

j = current density at 400 mV overpotential

M = molar mass of active materials

m = mass loading of a catalyst

F = faraday constant,

5.7, 16.29, 12.8 and 9.4, (current densities at 400 mV) for **EK-a**, **EK-b**, **EK-c** and **EK-d**

For **EK-a**, **EK-b**, **EK-c** and **EK-d**

(Co is the active material and molar mass of which is 58.93)

For, **EK-a**, TOF = 0.0057*58.93/4*0.000205*96485 /0.5 = 0.004

For, **EK-b**, TOF = 0.01629*58.93/4*0.000205*96485 /0.5 = 0.012

For, **EK-c**, TOF = 0.0128*58.93/4*0.000205*96485 /0.5 = 0.009

For, **EK-d**, TOF = 0.0094*299.73/4*0.000205*96485 /0.5 = 0.007

Current normalization

j_{ECSA} = i/ECSA (i = current and ECSA= C_{dl}/C_s)

j_{BET} = i/BET (i = current and BET surface area)

References:

1. Baehr, A., Moon, G., & Tüysüz, H. *Nitrogen-Doped Mesostructured Carbon Supported Metallic Cobalt Nanoparticles for Oxygen Evolution Reaction. ACS Applied Energy Materials,* **2019**, *2*, 9, 6672–6680. DOI: 10.1021/acsaem.9b01183
2. Liang, Y., Li, Y., Wang, H., Zhou, J., Wang, J., Regier, T., & Dai, H. (2011). *Co3O4 nanocrystals on graphene as a synergistic catalyst for oxygen reduction reaction. Nature Materials,* **2011**, *10*(10), 780–786. DOI: 10.1038/nmat3087
3. Chen, Z., Wang, Q., Zhang, X., Lei, Y., Hu, W., Luo, Y., & Wang, Y. *N-doped defective carbon with trace Co for efficient rechargeable liquid electrolyte-/all-solid-state Zn-air batteries. Science Bulletin,* **2018**, *63*(9), 548–555. DOI: 10.1016/j.scib.2018.04.003
4. Liu, S., Wang, Z., Zhou, S., Yu, F., Yu, M., Chiang, C.-Y., … Qiu, J. *Metal-Organic-Framework-Derived Hybrid Carbon Nanocages as a Bifunctional Electrocatalyst for Oxygen Reduction and Evolution. Advanced Materials,* **2017**, *29*(31), 1700874-1700883. DOI: 10.1002/adma.201700874
5. Mao, S., Wen, Z., Huang, T., Hou, Y., & Chen, J. *High-performance bi-functional electrocatalysts of 3D crumpled graphene–cobalt oxide nanohybrids for oxygen reduction and evolution reactions. Energy Environ. Sci.,* **2014**, *7*(2), 609–616. DOI: 10.1039/c3ee42696c
6. Amiinu, I. S., Liu, X., Pu, Z., Li, W., Li, Q., Zhang, J., … Mu, S. *From 3D ZIF Nanocrystals to Co-N_x/C Nanorod Array Electrocatalysts for ORR, OER, and Zn-Air Batteries. Advanced Functional Materials,* **2017**, *28*(5), 1704638. DOI: 10.1002/adfm.201704638

7. Masa, J., Xia, W., Sinev, I., Zhao, A., Sun, Z., Grützke, S., … Schuhmann, W. *Mn_xO_y/NC and Co_xO_y/NC Nanoparticles Embedded in a Nitrogen-Doped Carbon Matrix for High-Performance Bifunctional Oxygen Electrodes. Angewandte Chemie International Edition,* **2014**, *53*(32), 8508–8512. DOI: 10.1002/anie.201402710
8. Ma, T. Y., Dai, S., Jaroniec, M., & Qiao, S. Z. *Metal–Organic Framework Derived Hybrid Co_3O_4-Carbon Porous Nanowire Arrays as Reversible Oxygen Evolution Electrodes. Journal of the American Chemical Society,* **2014**, *136*(39), 13925–13931. DOI: 10.1021/ja5082553
9. Liu, X., Liu, W., Ko, M., Park, M., Kim, M. G., Oh, P., … Cho, J. *Metal (Ni, Co)-Metal Oxides/Graphene Nanocomposites as Multifunctional Electrocatalysts. Advanced Functional Materials,* **2015**, *25*(36), 5799–5808. DOI: 10.1002/adfm.201502217
10. Xiao, Q., Zhang, Y., Guo, X., Jing, L., Yang, Z., Xue, Y., … Sun, K. *A high-performance electrocatalyst for oxygen evolution reactions based on electrochemical post-treatment of ultrathin carbon layer coated cobalt nanoparticles. Chem. Commun.,* **2014**, *50*(86), 13019–13022. DOI: 10.1039/c4cc05953k
11. Wu, J., Xue, Y., Yan, X., Yan, W., Cheng, Q., & Xie, Y. *Co_3O_4 nanocrystals on single-walled carbon nanotubes as a highly efficient oxygen-evolving catalyst. Nano Research,* **2012**, *5*(8), 521–530. DOI: 10.1007/s12274-012-0237-y
12. Shi, Y., Wang, Y., Yu, Y., Niu, Z., & Zhang, B. *N-doped graphene wrapped hexagonal metallic cobalt hierarchical nanosheet as a highly efficient water oxidation electrocatalyst. Journal of Materials Chemistry A,* **2017**, *5*(19), 8897–8902. DOI: 10.1039/c7ta02838e
13. Cui, X., Ren, P., Deng, D., Deng, J., & Bao, X. *Single layer graphene encapsulating non-precious metals as high-performance electrocatalysts for water oxidation. Energy & Environmental Science,* **2016**, *9*(1), 123–129. DOI: 10.1039/c5ee03316k
14. Wang, J., Gao, D., Wang, G., Miao, S., Wu, H., Li, J., & Bao, X. *Cobalt nanoparticles encapsulated in nitrogen-doped carbon as a bifunctional catalyst for water electrolysis. J. Mater. Chem. A,* **2014**, *2*(47), 20067–20074. DOI: 10.1039/c4ta04337e.